Analytica Chimica Acta 1066 (2019) 102–111

Contents lists available at ScienceDirect

Analytica Chimica Acta

journal homepage: www.elsevier.com/locate/aca

Flow-through colorimetric assay for detection of nucleic acids in plasma

Gopal Ammanath [a, b, c, 1], Sanjida Yeasmin [a, c, 1], Yuvasri Srinivasulu [a, c], Mukti Vats [d], Jamal Ahmed Cheema [a, c], Fairuz Nabilah [a, c], Rohit Srivastava [d], Umit Hakan Yildiz [e], Palaniappan Alagappan [a, c, *], Bo Liedberg [a, c, **]

[a] Centre for Biomimetic Sensor Science, Nanyang Technological University, Singapore, 637553, Singapore
[b] NTU Institute for Health Technologies, Interdisciplinary Graduate School, Nanyang Technological University, Singapore, 637553, Singapore
[c] School of Materials Science and Engineering, Nanyang Technological University, Singapore, 639798, Singapore
[d] Department of Biosciences and Bioengineering, Indian Institute of Technology Bombay, Powai, Mumbai, 400076, India
[e] Department of Chemistry, Izmir Institute of Technology, Urla, 35430, Izmir, Turkey

HIGHLIGHTS

- A flow-through approach for multiplexed detection of nucleic acids in plasma samples is demonstrated.
- Unlike conventional assays, the proposed assay does not require tedious extraction or sample pre-treatment protocols.
- The assay yields colorimetric responses with good sensitivity and selectivity.
- A generalized logic system is proposed for profiling of nucleic acids.
- Assay possesses a great potential for rapid and point of care (POC) disease diagnosis in poor-resource settings.

GRAPHICAL ABSTRACT

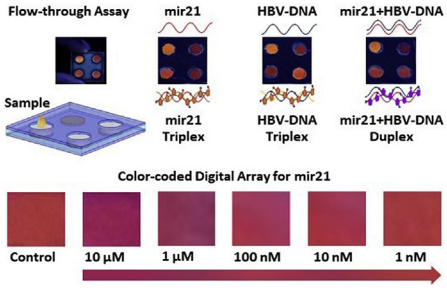

ARTICLE INFO

Article history:
Received 8 January 2019
Received in revised form
13 March 2019
Accepted 17 March 2019
Available online 19 March 2019

Keywords:
Colorimetric array
Polythiophene
Plasma
Nucleic acids
mir21
HBV-DNA

ABSTRACT

A flow-through colorimetric assay for detection of nucleic acids in plasma is reported. The proposed assay features an array of four polyvinylidene fluoride (PVDF) membranes impregnated with cationic poly (3-alkoxy-4-methylthiophene) (PT) as an optical reporter. The sensing strategy is based on monitoring the changes in optical properties of PT, upon complexation with target nucleic acids in the presence and in the absence of their corresponding complementary peptide nucleic acids (PNAs). As a proof of concept, the proposed methodology is validated using two biomarkers; lung cancer associated microRNA (mir21) and hepatitis B virus DNA (HBV-DNA). The flow-through colorimetric assay enabled detection of mir21 and HBV-DNA in plasma without requiring tedious sample pre-treatment and clean up protocols. Colorimetric responses for mir21 and HBV-DNA were obtained at nanomolar concentrations over five orders of magnitudes (from 1 nM to 10 μM), with a limit of detection of ~0.6 nM and ~2 nM in DI water and plasma, respectively. A logic gate system was developed to utilize the colorimetric assay responses as inputs for discrimination of mir21 and HBV-DNA and subsequently to obtain a profile of nucleic acids in samples that exceed respective clinical threshold limits, thereby enabling rapid and point

* Corresponding author. Centre for Biomimetic Sensor Science, Nanyang Technological University, Singapore, 637553, Singapore.
** Corresponding author. School of Materials Science and Engineering, Nanyang Technological University, Singapore, 639798, Singapore.
E-mail addresses: alps@ntu.edu.sg (P. Alagappan), bliedberg@ntu.edu.sg (B. Liedberg).
[1] Author contributed equally to this work.

https://doi.org/10.1016/j.aca.2019.03.036

of care (POC) disease diagnosis. Furthermore, the proposed methodology can be utilized for detection of a large number of nucleic acids in plasma by extending the array of PT impregnated membranes incorporated with their corresponding complementary PNAs.

1. Introduction

Nucleic acids have been realized as potential markers for diagnosis of metabolic (e.g., cancer) and infectious diseases (e.g., tuberculosis, hepatitis) [1–4]. Polymerase chain reaction (PCR) and microarray are commonly adopted techniques for nucleic acid assaying with good detection limits. These methodologies generally require instrumentation, trained personnel and are time-consuming, which prohibits the large-scale adoption [5–7]. Microfluidics and chip-based devices have therefore been explored in order to overcome these limitations; however, sophisticated fabrication protocols and external instrumentation may be required [8,9]. On the contrary, paper-based assays are facile, cost-effective, easy to use, enabling diagnosis in resource-limited settings [10–12].

Effort has been devoted to develop paper-based assays for rapid detection of nucleic acids [13,14]. However, clinical samples (e.g., plasma, serum, urine) are usually complex and contain trace amounts of the target nucleic acids of interest, therefore requiring tedious additional procedures such as isolation and sample pre-treatment for minimizing interferences from sample matrices. Most of the nucleic acids assays reported involve either extraction or amplification protocols, for instance, using extraction kits for isolation of nucleic acids prior to assaying [15,16]. In recent years, extraction and amplification processes have been integrated with paper-based assays [17–19]. These approaches involve longer assay time, multiple processing steps (e.g., interference exclusion and cleaning steps), and external functional units (e.g., heater and pressure supply) inhibiting point of care (POC) applications [8,20–22]. Since rapid and cost-effective assays are desirable, state-of-the art extraction processes involving tedious protocols may not be applicable for POC applications. Therefore, there is a need to develop alternative sample fractioning units such as membrane based filtering approaches. Herein, we report on a flow-through colorimetric assay for facile and multiplexed detection of nucleic acids in plasma samples, without requiring tedious extraction or pre-treatment protocols.

Colorimetric assays have drawn attention due to their quick visual response without requiring sophisticated instrumentation [23–28]. Various optical reporters such as gold nanoparticles, magnetic nanoparticles, carbon nanotubes, graphene oxide, and conjugated polymers (CPs) have been explored for colorimetric assaying [29]. Among these materials, CPs have been demonstrated to be very sensitive for nucleic acid assaying, predominantly in solution state, owing to their complexation capabilities with nucleic acids [30–41]. However, solution based assays are not robust as compared to paper-based assays due to the requirement of isolation steps and handling, and often suffers from low selectivity [42]. Previously, we have demonstrated a paper-based microRNA assay for naked-eye detection of lung cancer associated biomarker in buffer solutions, utilizing cationic polythiophene (PT) impregnated polyvinylidene fluoride (PVDF) membranes [43]. In the present report, we propose a flow-through approach for detection of nucleic acids in clinical samples in a multiplexed format. The proposed device features an array of PT impregnated PVDF membranes along with Fusion 5 filter papers and lamination sheets.

As a proof of concept, assay of two nucleic acid biomarkers, lung cancer associated biomarker microRNA (mir21) [44,45] and hepatitis B virus DNA (HBV-DNA) was performed. The sensing strategy, as illustrated in Fig. 1a, is based on monitoring the changes in optical properties of PT impregnated PVDF membrane, with and without peptide nucleic acid (PNA, complementary to corresponding target nucleic acid) upon complexation with target nucleic acid (mir21/HBV-DNA). PT without PNA forms a duplex with nucleic acids (PT-mir21 or/and PT-HBV-DNA) through electrostatic interactions between PT and nucleic acids, leading to a color change from orange to purple and to a fluorescence quenching according to the concentration of the nucleic acids. In contrary, PT with complementary PNA (PNA1, complementary for mir21 or PNA2, complementary for HBV-DNA) forms a triplex (PT-PNA1-mir21 or PT-PNA2-HBV-DNA) upon interaction with target nucleic acid, weakening electrostatic interaction between PT and mir21/HBV-DNA, and therefore does not yield significant color and fluorescence changes. The orange color (PT-PNA-mir21/HBV-DNA) and the significantly different purple color (PT-mir21/HBV-DNA) indicates the presence or absence of mir21/HBV-DNA in the sample, respectively, enabling colorimetric detection of nucleic acids. Experimental results illustrate a linear response between 1 nM and 10 μM, with a colorimetric limit of detection of ~0.6 nM and ~2 nM in DI water and plasma, respectively. The influence of the temperature and storage conditions are subsequently investigated for validation of the proposed nucleic acid assay for POC/on site applications. A generalized logic gate system has been developed for analysis of the colorimetric responses for rapid and selective screening of nucleic acids in plasma samples. The proposed methodology does not involve tedious extraction or sample pre-treatment protocols enabling POC detection of nucleic acids. This approach therefore enables POC multiplexed nucleic acid assay with high fidelity, which is of significant interest for progressive diagnostic and therapeutic applications [46–52].

2. Experimental section

2.1. Materials and chemicals

The centrifugal filters containing PVDF membranes with 0.1 μm pore size were purchased from Merck Millipore. Fusion 5 filters were obtained from Whatman. Human plasma was ordered from GeneTex, Taiwan. Fusion 5 is a hydrophilic filter paper prepared using a proprietary mix of glass fiber and polymer providing good wicking surface area and an optimal wicking time [53,54]. All the chemicals for PT synthesis were purchased from Sigma-Aldrich and used without further purification. The following nucleic acid sequences (mir21 and HBV-DNA) and PNA sequences were purchased from IDT (Singapore) and Panagene (Daejon, Korea), respectively.

mir21: 5′-UAG CUU AUC AGA CUG AUG UUG A-3′

HBV-DNA: 5′- TAT ATG GAT GAT GTG GTA TT -3′

PNA1: N-TCA ACA TCA GTC TGA TAA GCT A-C

PNA2: N-AAT ACC ACA TCA TCC ATA TA-C

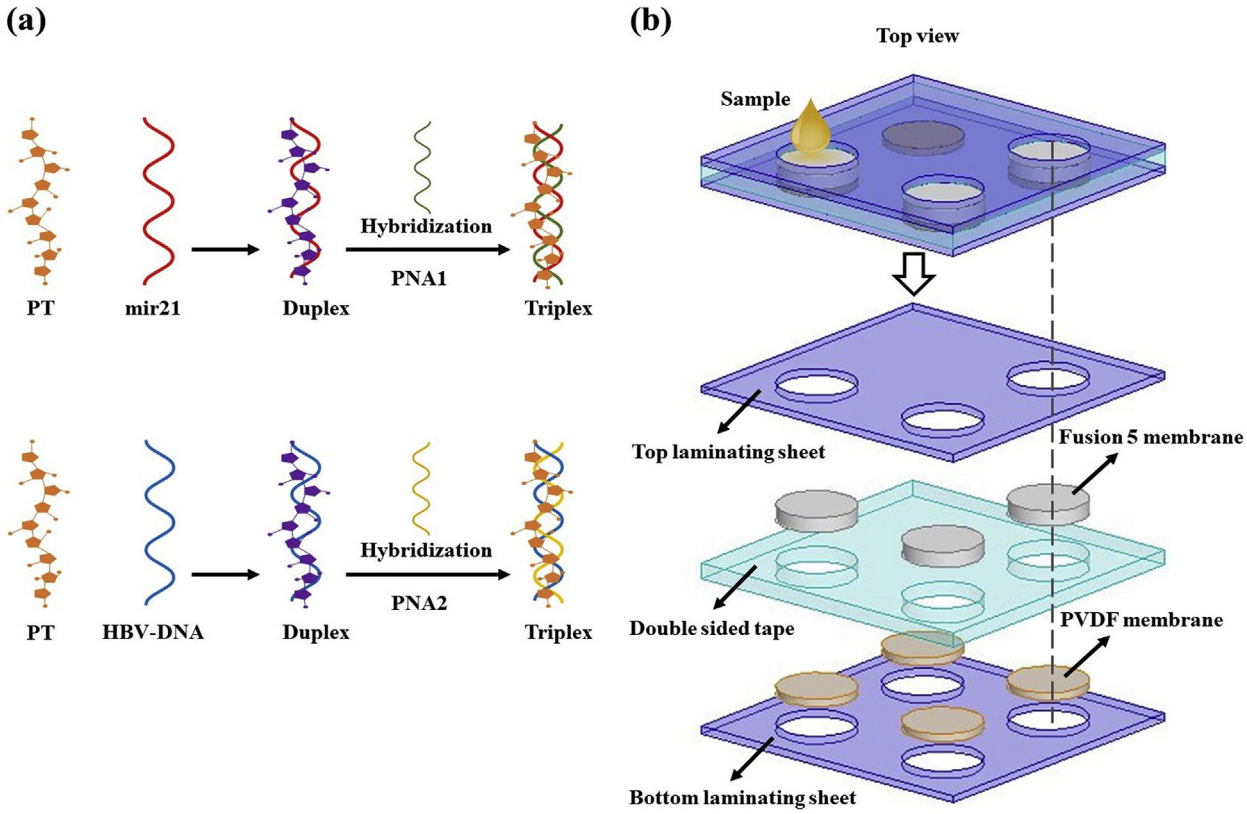

Fig. 1. Schematic illustration of (a) sensing strategy of mir21 and HBV-DNA through the duplex and triplex formation with PT in the absence and in the presence of their complementary PNAs and (b) flow-through device with four individually addressable PVDF membranes.

2.2. Synthesis, device fabrication and analysis

The synthesis and characterization of water-soluble cationic PT via oxidative polymerization have been described in detail in our previous report [55]. In brief, 200 μL of 1 μM PT was centrifuged with PVDF membranes in centrifugal tubes at 8000 rpm for 3 min. In order to obtain a homogenous coating of PT on PVDF membranes, the abovementioned step was repeated seven times, followed by washing with DI water under the same centrifugation conditions. Upon drying, the PT impregnated PVDF membranes were peeled off from the centrifugation tube for device fabrication upon ascertaining the homogeneity of PT on PVDF membranes via fluorescence spectroscopy and field emission scanning electronic microscopy (FESEM, Fig. S1). As shown in Fig. 1b, the device consists of an array of four PT impregnated PVDF membranes, three of them attached with Fusion 5 filter papers, stacked between two transparent lamination sheets. Fusion 5 filter paper acts as both a sample pad and as a membrane to filter macromolecules [53]. The transparent lamination sheets were used to encase the Fusion 5 and PVDF membrane as well as for handling the sensor. Double-sided adhesive tapes are utilized to secure the membranes to the laminated sheets.

PT impregnated PVDF membranes, numbered 1, 2, 3 and 4 as shown in Fig. 2a, are utilized as reference (membrane 1), for monitoring duplex response (membrane 2), for mir21 (membrane 3) and HBV-DNA (membrane 4) assaying, respectively. Membranes 3 and 4 were incubated with 25 μM complementary PNA (PNA1 and PNA2 for mir21 and HBV-DNA, respectively) for 45 min. For the assay, ~15 μL of samples spiked with varying concentrations of mir21/HBV-DNA was added on top of the Fusion 5 membrane. Herein, plasma was used as the clinical matrix with known concentrations of mir21/HBV-DNA. Plasma spiked with mir21/HBV-DNA concentrations [0 nM (control), 1 nM, 10 nM, 100 nM, 1 μM and 10 μM] were diluted 10 fold in DI water before the assay and was added to flow-through devices in the ambient conditions. The sample passively flows through the Fusion 5 membrane, which filters out macromolecules from the sample, allowing nucleic acids to reach the PT impregnated PVDF membrane. In order to observe the color changes of the PT impregnated PVDF membranes (membranes 2, 3 and 4, with respect to reference membrane 1) the flow-through device was placed under a portable UV lamp (UVL-28, 365 nm, 8 W) in a dark room. Digital images were then recorded with a mobile phone camera (Samsung S7), perpendicularly located over the device at a fixed distance. Subsequently, the captured digital images were imported to a computer in jpeg format for analysis using the ImageJ software. 75×75 pixels of each PT impregnated PVDF membranes (average of three locations at the centroids of the images, as shown in Fig. S2) were utilized to generate RGB values [56]. The fluorescence intensities were measured with Avantes spectrofluorometer and the emission spectra were recorded using the spectroscopy software provided (AvaSoft 8.0).

3. Results and discussion

The proposed flow-through colorimetric assay was carried out by observing changes in optical properties of PT impregnated PVDF membranes, upon complexation with the target nucleic acid in the presence/absence of complementary PNA sequence. Initially, all four PVDF membranes are orange in color, which is the inherent color of the PT. PT also remains orange upon exposure to PNA as neutral PNA (both PNA1 and PNA2) does not interact with positively charged PT

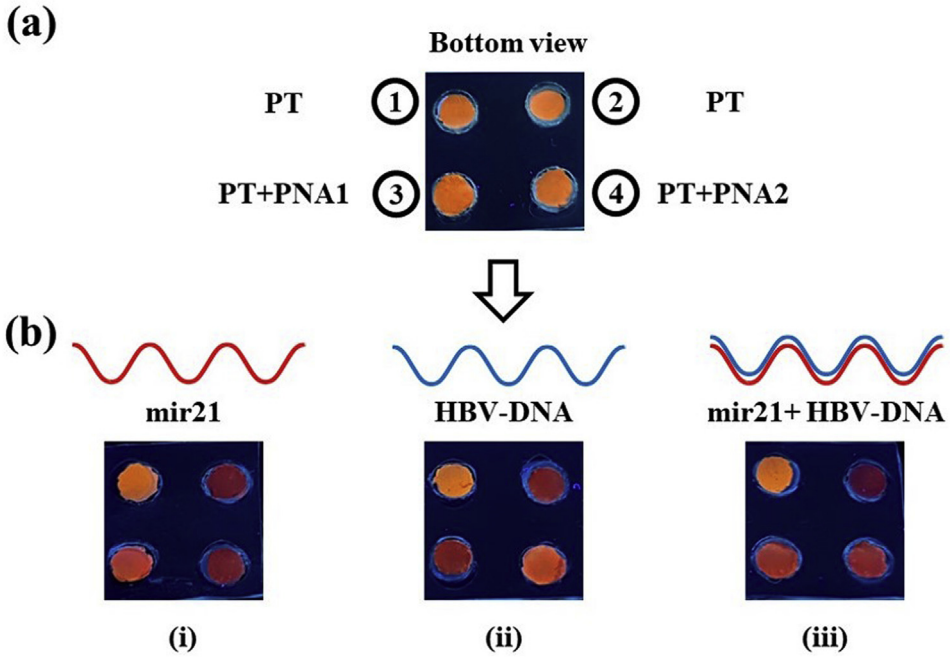

Fig. 2. Digital images of flow-through devices showing (a) colorimetric response of PT impregnated PVDF membranes (view from bottom) numbered 1, 2, 3 and 4 employed as reference (membrane 1), for monitoring duplex response (membrane 2), for mir21 (membrane 3) and HBV-DNA (membrane 4) assaying, respectively. (b) Colorimetric responses of PT impregnated PVDF membranes upon introducing (i) only mir21, (ii) only HBV-DNA and (iii) a mixture of mir21 and HBV-DNA.

[38]. 1 μM of PT and 25 μM of PNA (PNA1/PNA2) were experimentally found to be the optimum concentrations for assaying nanomolar (nM) concentrations of nucleic acids. As observed from Fig. 2b (i), with the addition of 1 μM mir21 to the flow through device (1 μM mir21 added to membranes 2, 3 and 4), a color change from orange to purple was observed for membranes 2 (PT) and membrane 4 (PT-PNA2, non-complementary to mir21). The color changes could be attributed to the formation of 'PT-mir21' duplex due to the electrostatic interactions between the positively charged PT and the negatively charged mir21. The random coiled morphology of the PT changes to a planar π-stacking morphology, leading to a substantial quenching of the fluorescence signal and color transition from orange to purple [56]. On the contrary, no significant color change (similar to the reference, membrane 1) was observed for the membrane 3 (PT-PNA1, complementary to mir21) due to the formation of a 'PT-PNA1-mir21' triplex structures. PT retains its random coiled morphology, owing to the hybridization between mir21 and PNA1, thereby retaining the fluorescence signal upon PT-PNA1-mir21 triplex formation. Similarly, with the addition of 1 μM HBV-DNA (Fig. 2b(ii)) to membranes 2, 3 and 4, purple color representing the duplex formation was observed on membranes 2 and 3, whereas, orange color representing the triplex formation was observed on membrane 4 (PT-PNA2-HBV-DNA). Subsequently, responses were evaluated for simultaneous detection both the markers using a mixture of mir21 (1 μM) and HBV-DNA (1 μM) added to membrane 2, 3 and 4. A dark purple color was observed on membrane 2, indicating significant duplex formation, as both mir21 and HBV-DNA sequence interacts with PT. In contrast, membrane 3 displays a reddish-orange color due to the formation of both duplex (PT-HBV-DNA) and triplex (PT-PNA1-mir21) morphologies. In a similar way, membrane 4 shows a reddish-orange color. Thus, the difference in colorimetric response between membrane 2 and membrane 3 (or, membrane 4) further ascertains that an array of PT membranes could be utilized to estimate the presence of different nucleic acids in sample matrices. Detailed RGB analysis was then carried out utilizing digital images (Fig. 2b) for quantification of the nucleic acids.

Fig. 3a and Fig. 3b illustrate the color-coded digital array for mir21 assay in DI water and plasma, respectively, spiked with mir21 concentrations varying from 10 μM to 1 nM (from left to right). In both cases, for PT without PNA, mir21 concentration dependant color changes are obtained, indicating a direct correlation between extent of PT planarization with concentration of mir21 (duplex formation). On the contrary, for assay in DI and plasma, PNA1 immobilized PT membranes reveal no significant changes in color upon mir21 addition indicating efficient PNA1-mir21 hybridization that weakens PT-mir21 electrostatic interactions, at all mir21 test concentrations. However, the color of PT appeared as reddish-orange for sample without mir21, instead of orange (as observed for assay in DI), which could be attributed to the interactions of PT with the plasma components.

The normalized fluorescence spectra of PT incorporated PVDF membranes with the addition of various concentrations of mir21 in DI water and plasma are shown in Fig. 3c and d, respectively. Upon excitation at 420 nm, emission bands centred at 568 nm and 578 nm are observed for PT in DI and plasma, respectively. The intensity of PT-mir21 gradually decreases with increasing concentration of mir21, indicating significant quenching due to the duplex formation. The normalized fluorescence spectra of PT-PNA1 membranes exposed to different concentrations of mir21 appear almost identical to each other due to the efficient hybridization between mir21 and PNA1 resulting in a triplex formation (therefore only the 1 μM mir21 spectrum that corresponds to the concentration used for illustration of assay in Fig. 2b (i) is shown here). Fig. 3d reveals concentration dependent mir21 quenching in plasma, which concurs with the response in DI water. Delta-E (ΔE) values, a metric (ranging from 0 to 100: $\Delta E > 2$ is regarded as the threshold value for visual differentiation of colors) for perception of color differences were then calculated from RGB values (shown in Fig. S3) based on the International Commission of Illumination (CIE) 1976 algorithm [57]. Significant differences in ΔE values between the duplex (ranging between ~49 and ~7, for the entire test concentration range) and the triplex (ranging between ~10 and ~5) are evident. ΔE analysis ascertains that

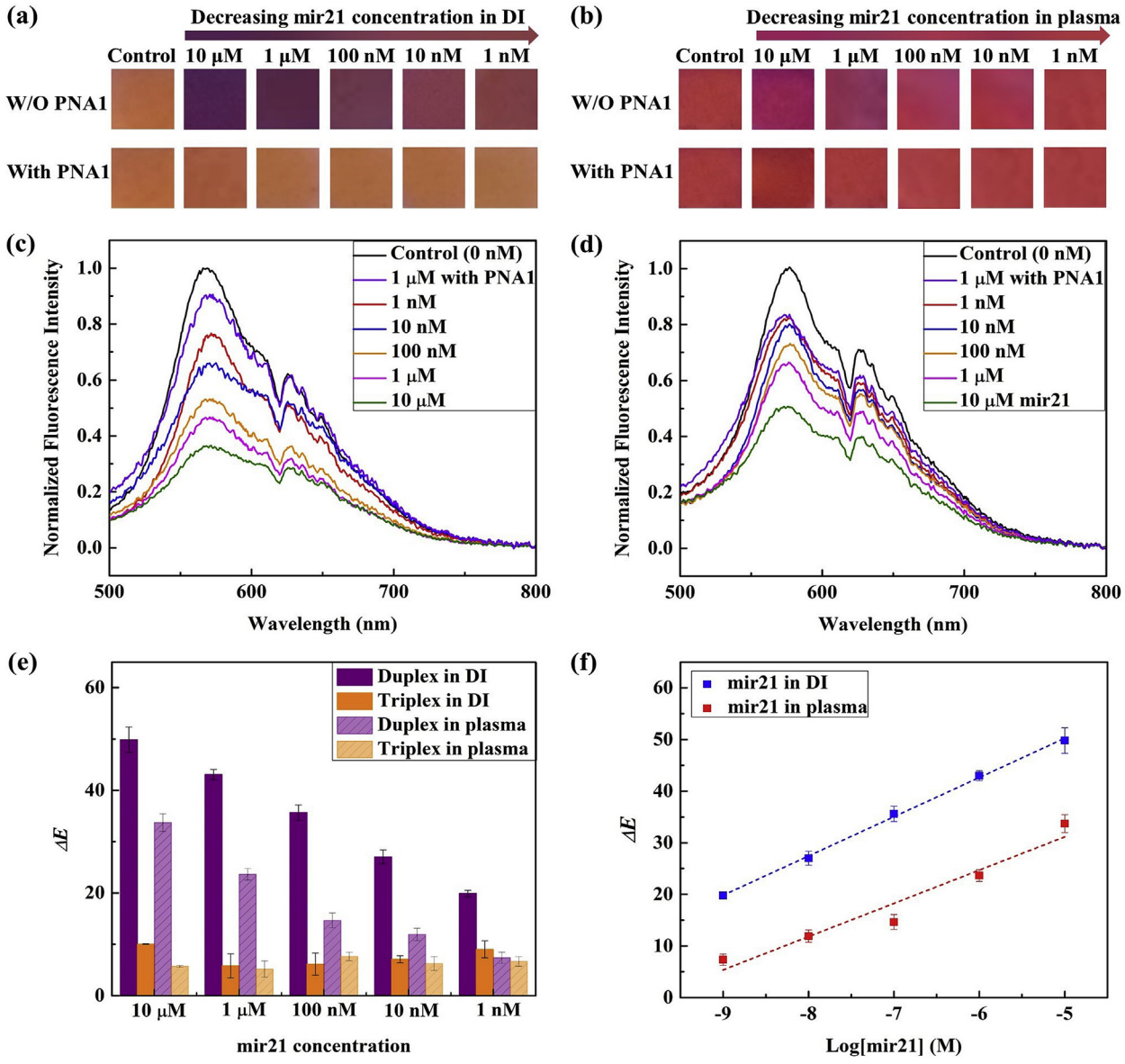

Fig. 3. Color-coded digital array of PT impregnated PVDF membranes (with/without PNA1) for various mir21 concentrations (10 μM to 1 nM) in (a) DI water, (b) plasma, and (c), (d) their corresponding fluorescence spectra, respectively. (e) Δ*E* values of duplex and triplex formation in both DI and plasma ($n = 3$). (f) Semi-logarithmic plot of the mir21 concentration versus Δ*E* in both DI and plasma ($n = 3$). (For interpretation of the references to color in this figure legend, the reader is referred to the Web version of this article.)

the color difference between duplex (PT-mir21) and triplex (PT-PNA1-mir21) is distinguishable and that the proposed assay could be utilized for the detection of mir21 in plasma over a wide dynamic range (1 nM−10 μM) as shown in Fig. 3e. The correlation between the Δ*E* values and mir21 concentrations was evaluated and represented in a semi-logarithmic scale, as shown in Fig. 3f. The data points in Fig. 3f is the average of Δ*E* values from three individual experiments. The calibration curves are linear over 5 orders of magnitude in both DI ($Y = 7.60\ log_{10}\ x + 88.24, R^2 = 0.99,\ n = 3$) and plasma ($Y = 6.44\ log_{10}\ x + 63.35, R^2 = 0.94,\ n = 3$) and limits of detection (LODs) in DI water and plasma are ~ 0.6 nM and ~2 nM, respectively (for a signal that is 3 times larger than the background noise), with an assay time of ~45 min. The error bars indicate that Δ*E* variations were less than 5% for $n = 3$.

Similarly, colorimetric responses for HBV-DNA between 10 μM and 1 nM concentration ranges spiked in both DI water and plasma are illustrated in Fig. 4 (a, b). The fluorescence spectra, Fig. 4c and d, shows similar quenching behaviour as compared to that of mir21. Further confirmation of detection is evident from the Δ*E* values (Fig. 4e), which displays considerable difference between duplex and triplex formation. LODs of ~0.6 nM and ~2 nM are achieved with calibration curves in DI water ($Y = 7.48\ log_{10}\ x + 86.53, R^2 = 0.99,\ n = 3$) and plasma ($Y = 5.16\ log_{10}\ x + 51.64, R^2 = 0.95,\ n = 3$), respectively (Fig. 4f), again with an assay time of ~45 min. In both cases, the trend of the HBV-DNA detection remains similar to that of mir21, which indicates that the proposed assay can be applied for the detection of any nucleic acid sequence in plasma. It should be noted that the color alteration was not easily perceptible for lower concentrations in plasma thus the exploration of *ΔE* values is recommended. In this work, 10 fold diluted plasma is used for evaluation of colorimetric responses of nucleic acids. Preliminary results on colorimetric responses for mir21 assay (concentrations down to 100 nM) in undiluted plasma samples are shown in Fig. S4. However, further

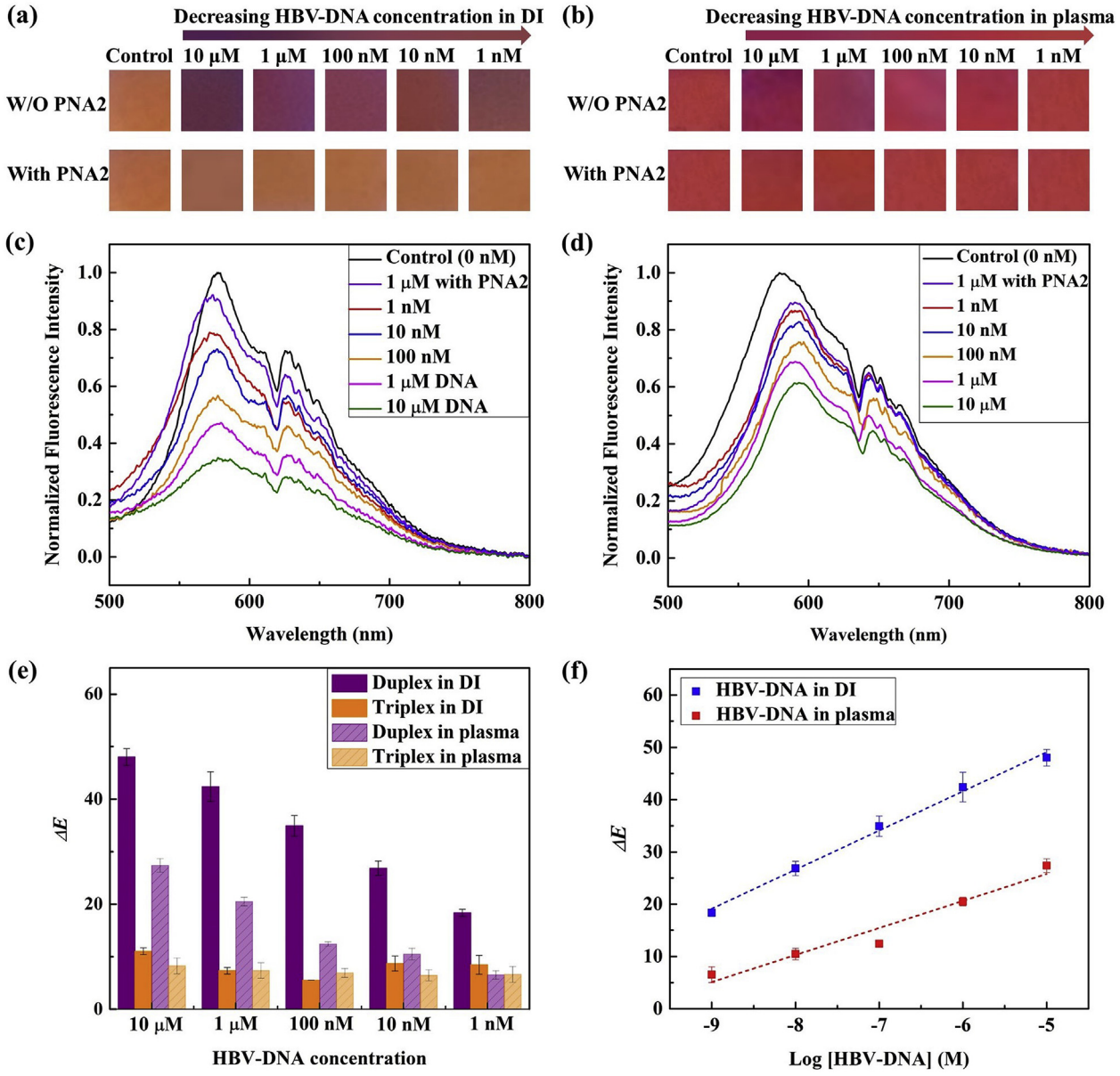

Fig. 4. Color-coded digital array of PT impregnated PVDF membranes (with/without PNA2) for various HBV-DNA concentrations (10 μM to 1 nM) in (a) DI water, (b) plasma, and (c), (d) their corresponding fluorescence spectra, respectably. (e) Δ*E* values of duplex and triplex formation in both DI and plasma ($n = 3$). (f) Semi-logarithmic plot of the HBV-DNA concentration versus Δ*E* in both DI and plasma ($n = 3$). (For interpretation of the references to color in this figure legend, the reader is referred to the Web version of this article.)

optimization in flow-through device architecture and PT deposition protocols would enable assaying low concentration of nucleic acids in undiluted plasma samples. LODs were also calculated from the fluorescence responses for both biomarkers to equal ~0.5 nM and ~1 nM in DI water and plasma, respectively (shown in Fig. S5).

3.1. Stability of the flow-through device

The influence of temperature and storage time on the stability of the flow-through device was then evaluated. The device was stored up to one month at varying temperatures (−20 °C, 4 °C, 10 °C, RT, and 30 °C). As PT is photosensitive, devices were stored in dark to prevent PT degradation (reduction in fluorescence intensity). Fig. 5a and Fig. 5b represent the color-coded digital array and the RGB responses of the devices that are freshly prepared and stored for one month at different temperatures, respectively. The color-coded images illustrate that the devices stored at 10 °C and RT are most stable among the different temperature ranges tested, as no significant color differences of PT membranes are observed as shown in Fig. 5a. RGB analysis yields the smallest difference of ~0.09 in G/B ratio (G/B ratio is calculated for evaluating the colorimetric responses as significant variations in green and blue intensities were observed compared to red intensities) for the devices that stored at room temperature. The devices stored at other temperatures show substantially higher difference in G/B ratio. Color-coded digital array (Fig. 5c) shows that mir21 assay could be carried out with devices that are stored at different temperatures even after one month. However, for the temperature ranges tested, mir21 assay responses (RGB values, Fig. 5d) of the device stored at RT for one month shows the minimal deviation of ~0.05 in G/B ratio from the responses obtained using freshly prepared devices, indicating that devices should be stored preferably at RT. Temperatures

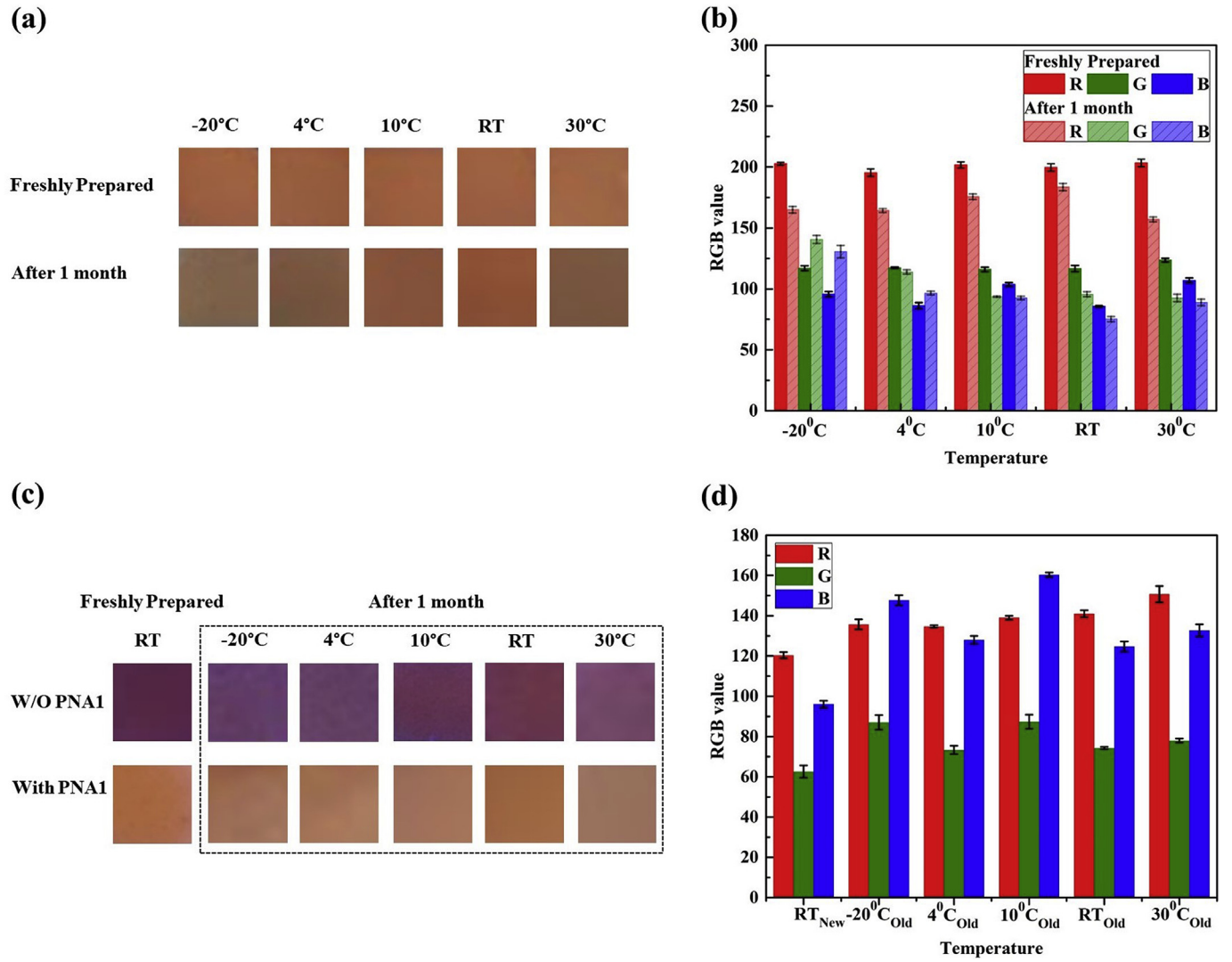

Fig. 5. (a) The colorimetric responses of freshly prepared and membranes stored for one month at varying temperatures (−20 °C, 4 °C, 10 °C, RT, 30 °C) and corresponding (b) RGB analysis ($n = 2$). (c) The colorimetric responses of 1 μM mir21 detection with freshly prepared and membranes stored for one month at varying temperatures and corresponding (d) RGB analysis (without PNA1, $n = 2$), (New-Freshly Prepared, Old-After 1 month).

over 30 °C (even for freshly prepared samples) are not suitable for storage of the devices due to degradation in the color and fluorescence intensity of PT.

3.2. Logic gate based nucleic acid computing

A generalized logic gate computing system for obtaining a profile of nucleic acids in sample is proposed. The colorimetric responses are utilized as inputs for the proposed logic gate system. As described in Fig. 2a, membranes 1, 2, 3 and 4 are utilized as references, for monitoring duplex responses, for mir21 assaying and for HBV-DNA assaying, respectively. For generalization, extending the PT array yield membranes numbered 5, 6 …n, which could be utilized for assaying other nucleic acid sequences of interest, upon incorporating the corresponding PNA sequences. Therefore, colorimetric response of the membranes 2, 3, 4 …n, upon addition of sample (except membrane 1), yield ΔE values as ΔE_{Duplex}, $\Delta E_{Triplex-mir21}$, $\Delta E_{Triplex-HBV-DNA} \ldots E_{Triplex-n}$, respectively, with membrane 1 as reference. The ΔE values are subsequently applied to the logic system for obtaining a profile of nucleic acids in the sample. The logic gate system consists of operational amplifiers (OA) and AND gates. The OA is employed as comparator with a non-inverting ($E(+)$) and an inverting inputs ($E(-)$) and one output. OA generates an output based on the difference between the two input voltages. The OA yields a logic '1' when the input voltage $E(+)$ is greater than the reference voltage $E(-)$, and logic '0' when the $E(+)$ is less then $E(-)$. The AND logic gate implements the logical conjunction of two inputs. AND gate yields logic '1' as output if and only if both the inputs are logic '1'.

Here, OAs are used to indicate the presence or absence of any specific nucleic acids at concentrations above the respective nucleic acid's clinical threshold limits. In order to realize this decision, the degree of the duplex/triplex formation as indicated by the ΔE values are compared with pre-set threshold values $\Delta E_{TH-Duplex}$ and $\Delta E_{TH-Triplex}$, respectively. $\Delta E_{TH-Duplex}$ is the ΔE value obtained experimentally by adding the minimum concentration of a nucleic acid, among the n nucleic acids tested, that indicates a diseased state. $\Delta E_{TH-Triplex}$ is evaluated from the response of a sample containing a mixture of minimum concentration of target nucleic acid at a diseased condition and a maximum possible concentration of total nucleic acid biomarker in samples (assuming 1 μM). For OA_1, if ΔE_{Duplex} is greater than or equal to $\Delta E_{TH-Duplex}$, then duplex

formation is ascertained. For the subsequent OAs, if $\Delta E_{TH-Triplex}$, is greater or equal to the $\Delta E_{Triplex}$, then the presence of specific nucleic acids sequences is ascertained. The outputs of all these OAs subsequently serve as inputs for AND logic gates in order to execute logical conjunction with the output from OA_1. The output of an AND gate is true only when both the duplex and triplex formations are true.

For an illustration of the operation of the proposed logic gate system, OA_2 and OA_3 are assigned for assaying mir21 and HBV-DNA sequences, respectively. As illustrated in Fig. 6a, for samples containing only mir21, both OA_1 and OA_2 yield logic '1', when ΔE_{Duplex} is greater than $\Delta E_{TH-Duplex}$ and $\Delta E_{TH-Triplex}$ is greater than $\Delta E_{Triplex-mir21}$, respectively. If both inputs are true, AND_1 yields a final output as logic '1' ($D_1 = 1$) indicating the presence of mir21. On the other hand, due to the absence of HBV-DNA in the sample, OA_3 would yield a logic '0', as $\Delta E_{TH-Triplex} < \Delta E_{Triplex-HBV-DNA}$. In this case, one of the inputs of the AND_2 is false, yielding a final output as logic '0' ($D_2 = 0$, confirming the absence of HBV-DNA). Fig. 6b represents the truth table for dual biomarkers detection ($n = 2$) as illustrated in Fig. 2a. In order to confirm the reliability of the proposed logic gate computing system, several testing combinations were experimentally evaluated as shown in Fig. S6. The proposed logic gate system outputs a reliable decision for obtaining a profile of nucleic acids in samples that are over their respective clinical threshold values, thereby enabling rapid POC diagnostics.

3.3. Comparison with other sensing strategies

Biological fluids typically contain trace amounts of nucleic acid biomarkers, and for instance, healthy human plasma contains nM level of specific sequences of microRNAs and up to few μM of microRNA in total [58,59]. Efforts have been devoted to detect these nucleic acid biomarkers in biological fluids such as blood [60], serum [61], plasma [33,62] and cells [63]. PCR is the most established method of microRNAs detection; for instance, quantitative real-time PCR microRNA profiling in plasma samples is reported [64]. However, PCR assay holds a number of time-consuming steps including RNA isolation, pre-amplification, and dilution, and thus requires trained personnel for interpretation of assay response. Therefore this methodology may not be applicable for POC assaying [65]. On the other hand, electrochemical, optical, capillary-electrophoresis and nanostructured materials-based methodologies have been reported for nucleic acid biomarker detection with good sensitivity. However, most of them require resources such as labelled probes, specialized fabrication protocols and sophisticated instrumentation for assaying [6]. These methods also require tedious sample pre-treatment. For example, an electrochemical sensor is reported for mir21 detection in human cells with a LOD of 0.4 pM requires dual labelling, a lab-based electrochemical workstation as well as RNA extraction [66]. Other reports such as a visible and label-free colorimetric sensor based on graphene/gold

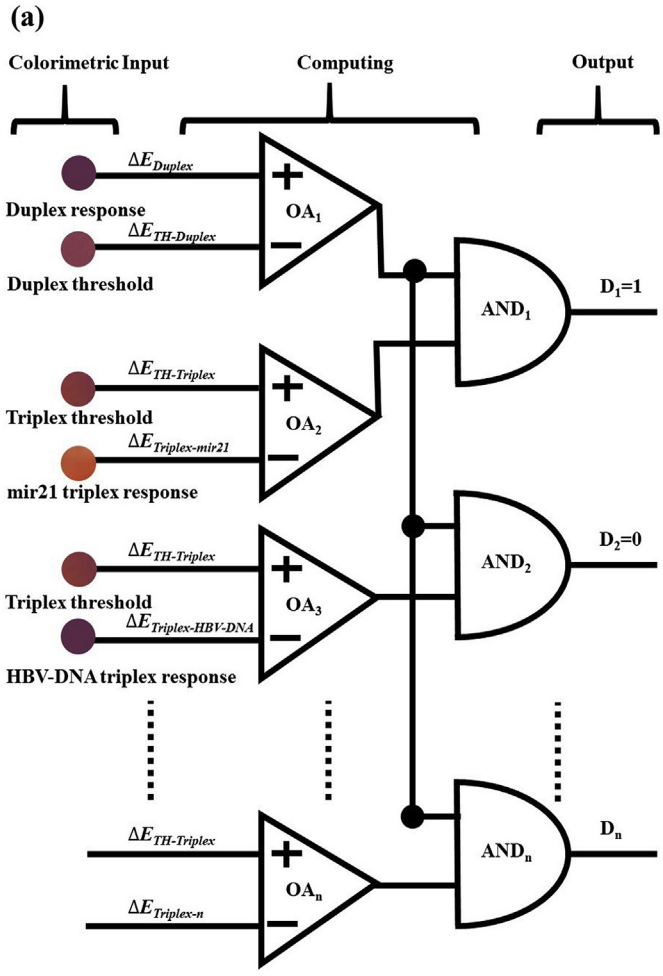

(b) Truth Table (n=2)

Op-Amp's input			AND's output		Possible clinical outcomes
Duplex	Triplex mir21	Triplex HBV-DNA	D_2	D_1	
			0	0	No disease
			0	1	Lung cancer related biomarker
			1	0	Hepatitis B virus biomarker
			1	1	Lung cancer & hepatitis B biomarker

Fig. 6. (a) A generalized nucleic acid biomarkers logic gate based system for specific detection of biomarkers from a mixture, illustrated using a truth table (b) for dual biomarkers ($n = 2$) detection.

nanoparticles hybrids detect mir21 in human serum with a LOD of ~3.2 nM [61] requires an additional approach such as protein/enzyme removal from serum through calefaction. Another colorimetric sensor reported for mir21 detection in plasma with cationic PT immobilized quartz resonator utilizes an extraction kit for isolation of mir21 [33]. In abovementioned cases, isolation of nucleic acids is required, which limits the POC applications. In this regard, the proposed flow-through assay eliminates tedious sample pre-treatment protocols, while offering detection of nucleic acids from plasma sample, upon dilution, with good sensitivity and specificity. The comparison of various colorimetric sensors for nucleic acids detection in clinical samples with the proposed approach is shown in Table S1. Furthermore, the fabrication of the flow-through device is facile, cost-effective, and highly reproducible, and it possesses a potential for multiplexed detection of nucleic acids upon extending the PT array and incorporating PNA that are complementary to the target nucleic acids. The assay shows good stability with time and temperature. Additionally, the logic gate system offers a reliable prediction of the disease for the samples containing target nucleic acids in clinically relevant concentrations, and therefore, has a great potential to facilitate rapid POC diagnostics in resource-limited settings.

4. Conclusion

A flow-through colorimetric assay is demonstrated for the detection of nucleic acids in plasma sample at concentrations over five orders of magnitudes. The integration of filter papers with the optical reporter (PT) incorporated PVDF membranes enable sample pre-treatment and detection in the same platform, thus improving the device robustness and functionality. The assay yields rapid detection of nucleic acids with good sensitivity and specificity, which can be employed for the early diagnosis of nucleic acid biomarkers related diseases. Colorimetric responses evaluated with RGB/ΔE analysis provide LOD in the low nM regime for both the mir21 and HBV-DNA in ~45 min. The generalized logic system offers a promising approach for profiling of colorimetric responses of nucleic acids. Therefore, the proposed methodology possesses a great potential for POC diagnostics.

Declaration of interests

The authors declare that they have no known competing financial interests or personal relationships that could have appeared to influence the work reported in this paper.

Appendix A. Supplementary data

Supplementary data to this article can be found online at https://doi.org/10.1016/j.aca.2019.03.036.

References

[1] U. Bora, A. Sett, D. Singh, Nucleic acid based biosensors for clinical applications, Biosens. J. 2 (1) (2013) 1–8.
[2] P. Craw, W. Balachandran, Isothermal nucleic acid amplification technologies for point-of-care diagnostics: a critical review, Lab Chip 12 (14) (2012) 2469–2486.
[3] A.C.-H. Yu, G. Vatcher, X. Yue, Y. Dong, M.H. Li, P.H. Tam, P.Y. Tsang, A.K. Wong, M.H. Hui, B. Yang, Nucleic acid-based diagnostics for infectious diseases in public health affairs, Front. Med. 6 (2) (2012) 173–186.
[4] N.L. Rosi, C.A. Mirkin, Nanostructures in biodiagnostics, Chem. Rev. 105 (4) (2005) 1547–1562.
[5] F. Chen, M. Lin, Y. Zhao, Y. Zhao, Catalase-functionalized SiO 2 nanoparticles mediate growth of gold nanoparticles for plasmonic biosensing of attomolar microRNA with the naked eye, RSC Adv. 6 (19) (2016) 15709–15715.
[6] T. Tian, J. Wang, X. Zhou, A review: microRNA detection methods, Org. Biomol. Chem. 13 (8) (2015) 2226–2238.
[7] A.C. Ghani, D.H. Burgess, A. Reynolds, C. Rousseau, Expanding the role of diagnostic and prognostic tools for infectious diseases in resource-poor settings, Nature 528 (7580) (2015) S50.
[8] J.R. Choi, R. Tang, S. Wang, W.A.B.W. Abas, B. Pingguan-Murphy, F. Xu, Paper-based sample-to-answer molecular diagnostic platform for point-of-care diagnostics, Biosens. Bioelectron. 74 (2015) 427–439.
[9] A. Nilghaz, D.H. Wicaksono, D. Gustiono, F.A.A. Majid, E. Supriyanto, M.R.A. Kadir, Flexible microfluidic cloth-based analytical devices using a low-cost wax patterning technique, Lab Chip 12 (1) (2012) 209–218.
[10] S. Kar, T.K. Maiti, S. Chakraborty, Microfluidics-based low-cost medical diagnostic devices: some recent developments, INAE Letters 1 (2) (2016) 59–64.
[11] W.G. Lee, Y.-G. Kim, B.G. Chung, U. Demirci, A. Khademhosseini, Nano/Microfluidics for diagnosis of infectious diseases in developing countries, Adv. Drug Deliv. Rev. 62 (4–5) (2010) 449–457.
[12] J.R. Choi, J. Hu, R. Tang, Y. Gong, S. Feng, H. Ren, T. Wen, X. Li, W.A.B.W. Abas, B. Pingguan-Murphy, An integrated paper-based sample-to-answer biosensor for nucleic acid testing at the point of care, Lab Chip 16 (3) (2016) 611–621.
[13] J. Hu, S. Wang, L. Wang, F. Li, B. Pingguan-Murphy, T.J. Lu, F. Xu, Advances in paper-based point-of-care diagnostics, Biosens. Bioelectron. 54 (2014) 585–597.
[14] X. Mao, H. Xu, Q. Zeng, L. Zeng, G. Liu, Molecular beacon-functionalized gold nanoparticles as probes in dry-reagent strip biosensor for DNA analysis, Chem. Commun. (21) (2009) 3065–3067.
[15] L.A. Rigano, M.R. Marano, A.P. Castagnaro, A.M. Do Amaral, A.A. Vojnov, Rapid and sensitive detection of Citrus Bacterial Canker by loop-mediated isothermal amplification combined with simple visual evaluation methods, BMC Microbiol. 10 (1) (2010) 176.
[16] L.A. Rigano, F. Malamud, I.G. Orce, M.P. Filippone, M.R. Marano, A.M. Do Amaral, A.P. Castagnaro, A.A. Vojnov, Rapid and sensitive detection of Candidatus Liberibacter asiaticus by loop mediated isothermal amplification combined with a lateral flow dipstick, BMC Microbiol. 14 (1) (2014) 86.
[17] B.A. Rohrman, R.R. Richards-Kortum, A paper and plastic device for performing recombinase polymerase amplification of HIV DNA, Lab Chip 12 (17) (2012) 3082–3088.
[18] J.C. Linnes, A. Fan, N.M. Rodriguez, B. Lemieux, H. Kong, C.M. Klapperich, Paper-based molecular diagnostic for Chlamydia trachomatis, RSC Adv. 4 (80) (2014) 42245–42251.
[19] N.M. Rodriguez, J.C. Linnes, A. Fan, C.K. Ellenson, N.R. Pollock, C.M. Klapperich, Paper-based RNA extraction, in situ isothermal amplification, and lateral flow detection for low-cost, rapid diagnosis of influenza A (H1N1) from clinical specimens, Anal. Chem. 87 (15) (2015) 7872–7879.
[20] Q. Wu, W. Jin, C. Zhou, S. Han, W. Yang, Q. Zhu, Q. Jin, Y. Mu, Integrated glass microdevice for nucleic acid purification, loop-mediated isothermal amplification, and online detection, Anal. Chem. 83 (9) (2011) 3336–3342.
[21] C.-H. Wang, K.-Y. Lien, J.-J. Wu, G.-B. Lee, A magnetic bead-based assay for the rapid detection of methicillin-resistant Staphylococcus aureus by using a microfluidic system with integrated loop-mediated isothermal amplification, Lab Chip 11 (8) (2011) 1521–1531.
[22] X. Fang, H. Chen, L. Xu, X. Jiang, W. Wu, J. Kong, A portable and integrated nucleic acid amplification microfluidic chip for identifying bacteria, Lab Chip 12 (8) (2012) 1495–1499.
[23] X. Ye, H. Shi, X. He, K. Wang, D. He, L.a. Yan, F. Xu, Y. Lei, J. Tang, Y. Yu, Iodide-responsive Cu–Au nanoparticle-based colorimetric platform for ultrasensitive detection of target cancer cells, Anal. Chem. 87 (14) (2015) 7141–7147.
[24] W. Zhao, M.A. Brook, Y. Li, Design of gold nanoparticle-based colorimetric biosensing assays, Chembiochem 9 (15) (2008) 2363–2371.
[25] R. Jelinek, S. Kolusheva, Biomolecular Sensing with Colorimetric Vesicles, Creative Chemical Sensor Systems, Springer, 2007, pp. 155–180.
[26] Y. Ding, B. Yang, H. Liu, Z. Liu, X. Zhang, X. Zheng, Q. Liu, FePt-Au ternary metallic nanoparticles with the enhanced peroxidase-like activity for ultrafast colorimetric detection of H2O2, Sensor. Actuator. B Chem. 259 (2018) 775–783.
[27] K. Wu, X. Zhao, M. Chen, H. Zhang, Z. Liu, X. Zhang, X. Zhu, Q. Liu, Synthesis of well-dispersed Fe 3 O 4 nanoparticles loaded on montmorillonite and sensitive colorimetric detection of H 2 O 2 based on its peroxidase-like activity, New J. Chem. 42 (12) (2018) 9578–9587.
[28] W. He, L. Luo, Q. Liu, Z. Chen, Colorimetric sensor array for discrimination of heavy metal ions in aqueous solution based on three kinds of thiols as receptors, Anal. Chem. 90 (7) (2018) 4770–4775.
[29] Y. Song, W. Wei, X. Qu, Colorimetric biosensing using smart materials, Adv. Mater. 23 (37) (2011) 4215–4236.
[30] S.W. Thomas, G.D. Joly, T.M. Swager, Chemical sensors based on amplifying fluorescent conjugated polymers, Chem. Rev. 107 (4) (2007) 1339–1386.
[31] T.M. Swager, The molecular wire approach to sensory signal amplification, Acc. Chem. Res. 31 (5) (1998) 201–207.
[32] L. Chen, D.W. McBranch, H.-L. Wang, R. Helgeson, F. Wudl, D.G. Whitten, Highly sensitive biological and chemical sensors based on reversible fluorescence quenching in a conjugated polymer, Proc. Natl. Acad. Sci. Unit. States Am. 96 (22) (1999) 12287–12292.
[33] A. Palaniappan, J.A. Cheema, D. Rajwar, G. Ammanath, L. Xiaohu, L.S. Koon, W. Yi, U.H. Yildiz, B. Liedberg, Polythiophene derivative on quartz resonators for miRNA capture and assay, Analyst 140 (23) (2015) 7912–7917.
[34] H.-A. Ho, A. Najari, M. Leclerc, Optical detection of DNA and proteins with cationic polythiophenes, Accounts Chem. Res. 41 (2) (2008) 168–178.
[35] B. Liu, G.C. Bazan, Homogeneous fluorescence-based DNA detection with

water-soluble conjugated polymers, Chem. Mater. 16 (23) (2004) 4467–4476.
[36] W. Zheng, L. He, Label-free, real-time multiplexed DNA detection using fluorescent conjugated polymers, J. Am. Chem. Soc. 131 (10) (2009) 3432–3433.
[37] K.P.R. Nilsson, O. Inganäs, Chip and solution detection of DNA hybridization using a luminescent zwitterionic polythiophene derivative, Nat. Mater. 2 (6) (2003) 419.
[38] H. Jiang, P. Taranekar, J.R. Reynolds, K.S. Schanze, Conjugated polyelectrolytes: synthesis, photophysics, and applications, Angew. Chem. Int. Ed. 48 (24) (2009) 4300–4316.
[39] Y. Zhang, Z. Li, Y. Cheng, X. Lv, Colorimetric detection of microRNA and RNase H activity in homogeneous solution with cationic polythiophene derivative, Chem. Commun. (22) (2009) 3172–3174.
[40] H.A. Ho, M. Boissinot, M.G. Bergeron, G. Corbeil, K. Doré, D. Boudreau, M. Leclerc, Colorimetric and fluorometric detection of nucleic acids using cationic polythiophene derivatives, Angew. Chem. 114 (9) (2002) 1618–1621.
[41] W. Zheng, T.E. Chase, L. He, Multiplexed miRNA detection using cationic polythiophene, Analytical Methods 6 (7) (2014) 2399–2405.
[42] K. Lee, L.K. Povlich, J. Kim, Recent advances in fluorescent and colorimetric conjugated polymer-based biosensors, Analyst 135 (9) (2010) 2179–2189.
[43] U.H. Yildiz, P. Alagappan, B. Liedberg, Naked eye detection of lung cancer associated miRNA by paper based biosensing platform, Anal. Chem. 85 (2) (2012) 820–824.
[44] J. Wei, W. Gao, C.-J. Zhu, Y.-Q. Liu, Z. Mei, T. Cheng, Y.-Q. Shu, Identification of plasma microRNA-21 as a biomarker for early detection and chemosensitivity of non–small cell lung cancer, Chin. J. Canc. 30 (6) (2011) 407.
[45] W. Zheng, J. Zhao, Y. Tao, M. Guo, Z. Ya, C. Chen, N. Qin, J. Zheng, J. Luo, L. Xu, MicroRNA-21: a promising biomarker for the prognosis and diagnosis of non-small cell lung cancer, Oncology letters 16 (3) (2018) 2777–2782.
[46] Y.-H. Lai, S.-C. Sun, M.-C. Chuang, Biosensors with built-in biomolecular logic gates for practical applications, Biosensors 4 (3) (2014) 273–300.
[47] C. Wu, S. Wan, W. Hou, L. Zhang, J. Xu, C. Cui, Y. Wang, J. Hu, W. Tan, A survey of advancements in nucleic acid-based logic gates and computing for applications in biotechnology and biomedicine, Chem. Commun. 51 (18) (2015) 3723–3734.
[48] E. Katz, J. Wang, M. Privman, J. Halámek, Multianalyte Digital Enzyme Biosensors with Built-In Boolean Logic, ACS Publications, 2012.
[49] E. Katz, Biomolecular Information Processing: from Logic Systems to Smart Sensors and Actuators, John Wiley & Sons, 2013.
[50] J. Wang, E. Katz, Digital biosensors with built-in logic for biomedical applications—biosensors based on a biocomputing concept, Anal. Bioanal. Chem. 398 (4) (2010) 1591–1603.
[51] E. Katz, Molecular and Supramolecular Information Processing: from Molecular Switches to Logic Systems, John Wiley & Sons, 2013.
[52] E. Katz, V. Privman, Enzyme-based logic systems for information processing, Chem. Soc. Rev. 39 (5) (2010) 1835–1857.
[53] J. Linnes, N. Rodriguez, L. Liu, C. Klapperich, Polyethersulfone improves isothermal nucleic acid amplification compared to current paper-based diagnostics, Biomed. Microdevices 18 (2) (2016) 30.
[54] S. Hosseini, P. Vázquez-Villegas, S.O. Martínez-Chapa, Paper and fiber-based bio-diagnostic platforms: current challenges and future needs, Appl. Sci. 7 (8) (2017) 863.
[55] D. Rajwar, G. Ammanath, J.A. Cheema, A. Palaniappan, U.H. Yildiz, B. Liedberg, Tailoring conformation-induced chromism of polythiophene copolymers for nucleic acid assay at resource limited settings, ACS Appl. Mater. Interfaces 8 (13) (2016) 8349–8357.
[56] G. Ammanath, U.H. Yildiz, A. Palaniappan, B. Liedberg, Luminescent device for the detection of oxidative stress biomarkers in artificial urine, ACS Appl. Mater. Interfaces 10 (9) (2018) 7730–7736.
[57] B. Hill, T. Roger, F.W. Vorhagen, Comparative analysis of the quantization of color spaces on the basis of the CIELAB color-difference formula, ACM Trans. Graph. 16 (2) (1997) 109–154.
[58] H.M. Heneghan, N. Miller, M.J. Kerin, Circulating miRNA signatures: promising prognostic tools for cancer, J. Clin. Oncol. 28 (29) (2010) e573–e574.
[59] J.A. Weber, D.H. Baxter, S. Zhang, D.Y. Huang, K.H. Huang, M.J. Lee, D.J. Galas, K. Wang, The microRNA spectrum in 12 body fluids, Clin. Chem. 56 (11) (2010) 1733–1741.
[60] X. Lu, X. Dong, K. Zhang, X. Han, X. Fang, Y. Zhang, A gold nanorods-based fluorescent biosensor for the detection of hepatitis B virus DNA based on fluorescence resonance energy transfer, Analyst 138 (2) (2013) 642–650.
[61] H. Zhao, Y. Qu, F. Yuan, X. Quan, A visible and label-free colorimetric sensor for miRNA-21 detection based on peroxidase-like activity of graphene/gold-nanoparticle hybrids, Analytical Methods 8 (9) (2016) 2005–2012.
[62] Y. Liu, M. Wei, Y. Li, A. Liu, W. Wei, Y. Zhang, S. Liu, Application of spectral crosstalk correction for improving multiplexed MicroRNA detection using a single excitation wavelength, Anal. Chem. 89 (6) (2017) 3430–3436.
[63] N. Lu, A. Gao, P. Dai, S. Song, C. Fan, Y. Wang, T. Li, CMOS-compatible silicon nanowire field-effect transistors for ultrasensitive and label-free microRNAs sensing, Small 10 (10) (2014) 2022–2028.
[64] A.B. Gevaert, I. Witvrouwen, C.J. Vrints, H. Heidbuchel, E.M. Van Craenenbroeck, S.J. Van Laere, A.H. Van Craenenbroeck, MicroRNA profiling in plasma samples using qPCR arrays: recommendations for correct analysis and interpretation, PLoS One 13 (2) (2018), e0193173.
[65] L. Vaca, Point-of-care diagnostic tools to detect circulating microRNAS as biomarkers of disease, Sensors 14 (5) (2014) 9117–9131.
[66] Y. Zhou, Z. Zhang, Z. Xu, H. Yin, S. Ai, MicroRNA-21 detection based on molecular switching by amperometry, New J. Chem. 36 (10) (2012) 1985–1991.